The Astrophysical Journal Letters, 1004:L41 (7pp), 2026 June 20 https://doi.org/10.3847/2041-8213/ae77e5

From One to Two: A Second Binary Millisecond Pulsar in the Globular Cluster M92 (NGC 6341)

Dejiang Yin[1], Li-yun Zhang[1,2,3], Baoda Li[1], Yinfeng Dai[4,5], Lin Wang[6], Qiuyu Yu[1,7], and Yujie Lian[5]
[1] College of Physics, Guizhou University, Guiyang 550025, People's Republic of China; liy_zhang@hotmail.com
[2] Guizhou Radio Astronomical Observatory, Guizhou University, Guiyang 550025, People's Republic of China
[3] International Centre of Supernovae, Yunnan Key Laboratory, Kunming 650216, People's Republic of China
[4] Institute for Frontier in Astronomy and Astrophysics & Faculty of Arts and Sciences, Beijing Normal University, Zhuhai 519087, People's Republic of China
[5] School of Physics and Astronomy, Beijing Normal University, Beijing 100875, People's Republic of China
[6] State Key Laboratory of Radio Astronomy and Technology, Shanghai Astronomical Observatory, Chinese Academy of Sciences, 80 Nandan Road, Shanghai 200030, People's Republic of China
[7] Guizhou Vocational College of Foodstuff Engineering, Guiyang 550025, People's Republic of China
Received 2026 April 18; revised 2026 May 27; accepted 2026 June 2; published 2026 June 18

Abstract

We report the discovery and phase-connected timing solution of a second millisecond binary pulsar, PSR J1717 +4308B (M92B), in the globular cluster M92 (NGC 6341) using the Five-hundred-meter Aperture Spherical radio Telescope. This new pulsar, with a spin period of 3.51 ms and a dispersion measure (DM) of 35.29 pc cm^{-3}, was discovered through frequency-domain acceleration searches. The timing solution shows that M92B is in a binary system with an orbital period of 2.3 days, an eccentricity of $\simeq 4.8 \times 10^{-4}$, and a minimum companion mass of 0.2 $M_{\odot}$. M92B lies within the cluster core radius in projection, and its negative spin period derivative ($\dot{P}$) is consistent with acceleration in the cluster potential. The measured negative $\dot{P}$ of M92B, together with a DM consistent with that of M92A (<0.2 pc cm^{-3}), confirms that both pulsars are members of the cluster. A Bayesian Markov Chain Monte Carlo analysis based on these two pulsars yields broad constraints on the core structural parameters of M92 that are consistent with *N*-body dynamical modeling. This demonstrates that pulsar timing can provide useful dynamical information in sparse pulsar samples.

Unified Astronomy Thesaurus concepts: Globular star clusters (656); Millisecond pulsars (1062); Radio telescopes (1360)

1. Introduction

Globular clusters (GCs) are favorable environments for producing millisecond pulsars (MSPs) owing to their extremely high stellar densities ($\gtrsim 10^3\ M_{\odot}$ pc^{-3}; W. E. Harris 2010) compared to the Galactic field (G. W. Clark 1975; M. A. Alpar et al. 1982). Pulsars in GCs[9] include extreme systems such as the fastest-spinning pulsar (J. W. T. Hessels et al. 2006) and candidate pulsar–black hole binaries (E. D. Barr et al. 2024), which are exclusive products of cluster dynamics and are rarely found in the Galactic disk. Beyond the study of individual exotic systems, a population of pulsars within a cluster can probe the properties of its host cluster, e.g., the gravitational potential and possible central intermediate-mass black holes (e.g., P. C. C. Freire et al. 2017; B. B. P. Perera et al. 2017; A. Corongiu et al. 2024), and intracluster magnetic field and gas content (P. C. Freire et al. 2001; F. Abbate et al. 2018). Accordingly, given their rich scientific potential, GCs have long been prime targets for pulsar searches and studies (e.g., F. Camilo et al. 2000; S. M. Ransom et al. 2005; J. W. T. Hessels et al. 2007; Z. Pan et al. 2021; A. Ridolfi et al. 2021).

GC pulsars are typically faint radio sources located at significant distance (e.g., >2 kpc; W. E. Harris 2010), resulting in low observed flux densities (e.g., J. W. T. Hessels et al. 2007; Z. Pan et al. 2021; A. Ridolfi et al. 2021; Y. Lian et al. 2025). Most GC pulsars (∼93% of the total) are MSPs, and about 56% of the population reside in binary systems (S. M. Ransom 2008; D.-J. Yin et al. 2023). Orbital motion in binary systems modulates the pulsar signal, spreading the signal power over a range of frequencies and reducing the detectability of faint signals (D. R. Lorimer & M. Kramer 2004). However, interstellar scintillation can occasionally enhance the apparent flux density of pulsars above the detection threshold, enabling the detection of previously missed pulsars that were below survey sensitivity limits (e.g., M13G–I; Y. Li et al. 2025; D. Yin et al. 2025).

Empirical estimates of GC pulsar populations suggest that M92 is among the most promising targets for deep searches (see L. Zhang et al. 2016; Z. Pan et al. 2020) with the Five-hundred-meter Aperture Spherical radio Telescope (FAST; R. Nan et al. 2011; P. Jiang et al. 2020). The first pulsar in M92, PSR J1717+4308A (M92A), was discovered during an early observation of GC FANS[10] on 2017 October 9 (Z. Pan et al. 2020). M92A is a 3.15 ms MSP in an eclipsing "redback" binary with an orbital period of 4.8 hr. Its X-ray counterpart was identified and exhibits a luminosity of 8.3×10^{31} erg s^{-1} in the 0.3–8 keV band from Chandra observations (J. Zhao & C. O. Heinke 2022). The first phase-connected timing solution for M92A was obtained from timing observations in 2021 (Z. Pan et al. 2021) and recently updated in 2025 (Y. Lian et al. 2025). These data also provide an opportunity to search

[9] See the continuously updated catalog of GC pulsars maintained by P. C. C. Freire: https://www3.mpifr-bonn.mpg.de/staff/pfreire/GCpsr.html.

[10] Globular Cluster with FAST: A Neutron-star Survey; Z. Pan et al. (2021), Y. Lian et al. (2025).

for additional pulsars that may reside within the cluster (e.g., P. J. Turk & D. R. Lorimer 2013; D. Yin et al. 2024), whose discovery would provide further evidence for the association of M92A with M92 (Z. Pan et al. 2020).

In this Letter, we searched for additional pulsars in M92 using 6 yr of FAST timing observations for M92A. This extensive baseline significantly increased the chances of detecting faint pulsars that may occasionally become detectable due to interstellar scintillation. The structure of this Letter is as follows. Section 2 describes the FAST observations and data reduction. Section 3 presents the discovery and timing results of the new pulsar. Sections 4 and 5 provide a brief discussion and summary.

2. Observation and Data Reduction

2.1. FAST Observation

The early FAST observations of M92, together with the observing setup and initial data reduction, were described by Z. Pan et al. (2020, 2021). Here we analyze 25 observations obtained between 2019 June 25 and 2025 August 26. The integration times range from 1800 to 18,000 s. M92 has a core radius of $r_c = 0.'26$ and a half-light radius of $r_h = 1.'02$ (W. E. Harris 2010). Both are well within the $2.'9$ half-power beamwidth of the FAST 19-beam *L*-band receiver. The central beam was pointed at the cluster center (R.A. = 17:17:07.39, decl. = +43:08:09.4; W. E. Harris 2010) for all observations, and only the central-beam data were analyzed in this work. All data were taken over 1.0–1.5 GHz, channelized into 4096 channels of width 0.122 MHz (P. Jiang et al. 2019). These observations were carried out in the `Tracking` or `Swift-Calibration` mode with a sampling time of 49.152 μs and recorded in the standard search-mode PSRFITS format (A. W. Hotan et al. 2004).

2.2. Data Reduction

Pulsar searches were performed using the PULSAR EXPLORATION AND SEARCH TOOLKIT (PRESTO;[11] S. M. Ransom 2001; S. M. Ransom et al. 2002) package with the MOSS scripts[12] (D. Yin 2025). Radio-frequency interference was mitigated in both the time and frequency domains using the `rfifind` routine. Dedispersed time series were then generated from the PSRFITS data using `prepsubband` routine over a range of trial dispersion measures (DMs). The previously known pulsar in this cluster, M92A, has a DM of 35.45 pc cm^{-3} (Z. Pan et al. 2020). Following the empirical relation between the mean DM and DM spread of pulsars in GCs (D.-J. Yin et al. 2023), we searched a DM range broader than the expected spread around the known pulsar M92A (35.45 pc cm^{-3}), covering 32–38 pc cm^{-3} with a step size of 0.05 pc cm^{-3}. This DM step corresponds to a pulse broadening of only ∼2% for a minimum spin period of 0.5 ms considered in our search (J. W. T. Hessels et al. 2007).

The dedispersed time series were transformed to the fluctuation frequency domain using the `realfft` routine, and low-frequency red noise was mitigated with the `rednoise` routine. Fourier-domain acceleration searches were then performed with the `accelsearch` routine (S. M. Ransom et al. 2002). To enhance sensitivity to short-orbit systems, observations longer than 3000 s were divided into ∼1500–2500 s segments for acceleration searches according to the observing duration at each epoch. Acceleration searches were performed on both full-length observations and segmented data using harmonic summing up to 32. For computationally efficient searches of isolated pulsars and low-acceleration pulsars in long-orbit binaries, we used $z_{max} = 20$. For segmented data targeting accelerated pulsars in short-orbit binaries, we initially used $z_{max} = 300$, and later adopted $z_{max} = 520$ after the new discovery to improve sensitivity to more accelerated signals.

We also performed "jerk" searches on the segmented data to account for rapidly varying accelerations. Following the search setups explored by B. C. Andersen & S. M. Ransom (2018), we used $z_{max} = 100$ and $w_{max} = 500$, as well as a wider search with $z_{max} = 300$ and $w_{max} = 900$, both with four-harmonic summing.

All candidates produced by the `accelsearch` routine were sifted using a customized version of the `ACCEL_sift.py` script in PRESTO. Each diagnostic plot used for initial inspection comprises two panels, showing the folded profile of the dedispersed time series (upper) and the trial DM-detected significance curve (lower). Promising candidates were then refolded using the raw PSRFITS data to produce standard diagnostic plots for final verification.

Upon discovery of a binary pulsar, initial orbital parameters were obtained using the `fitorb.py` script in PRESTO, based on the apparent barycentric spin periods and their derivatives measured at different orbital phases. Using initial parameters, the data were folded to construct a preliminary timing model. Subsequent timing iterations refined the orbital solution, yielding more detections in observations where the pulsar signal is weak and affected by orbital modulation. A standard template profile was constructed from high signal-to-noise detections using Gaussian-component fitting with PRESTO's `pygaussfit.py` script. Pulse times of arrival (TOAs) were obtained with `get_TOA.py` script using the Fourier-domain template matching technique (J. H. Taylor 1992).

3. Results

3.1. Discovery and Timing of M92B

Our acceleration searches ($z_{max} = 300$ scheme) of the FAST monitoring observations revealed a new MSP in M92, PSR J1717+4308B (hereafter M92B, see Figure 1). The pulsar was detected with a spin period of 3.51 ms and a DM of 35.35 pc cm^{-3}, consistent with the DM of the previously known pulsar M92A. The discovery signal exhibited significant Doppler acceleration (∼0.2 m s^{-2}), suggesting that the pulsar is in a binary system. Figure 1 shows mild higher-order orbital effects in the acceleration-search discovery signal, corresponding to a small line-of-sight (LOS) jerk of $\sim 1.2 \times 10^{-5}$ m s^{-3}. No eclipses were detected for M92B in our observations.

The timing analysis was performed using the TEMPO[13] (D. Nice et al. 2015) and DRACULA[14] (P. C. C. Freire & A. Ridolfi 2018) packages, yielding a phase-connected timing solution with the ELL1 model (C. Lange et al. 2001). The

[11] https://github.com/scottransom/presto

[12] Multiple Observation Segment Search (MOSS) for Pulsars: https://github.com/ydejiang/MOSS; see details in D. Yin et al. (2025).

[13] https://tempo.sourceforge.net/

[14] https://github.com/pfreire163/Dracula

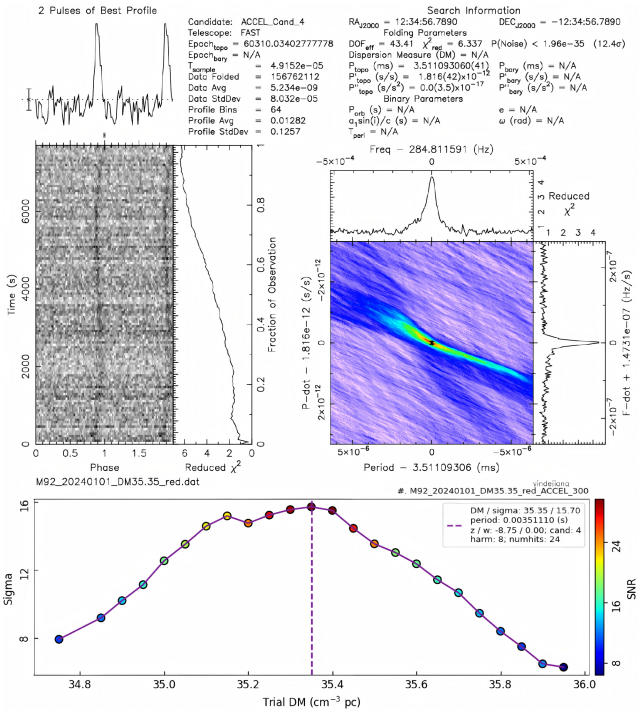

Figure 1. Discovery plot of M92B. Top: folded pulse profile from the dedispersed time series produced using `prepfold`. Bottom: detection significance as a function of trial DM, peaking near the optimal value and decreasing due to dispersive smearing.

timing results show that M92B is a binary MSP with an orbital period of 2.3 days and a mildly eccentricity of $e = 4.82(1) \times 10^{-4}$. The derived timing parameters are listed in Table 1, and the corresponding timing residuals are shown in Figure 2.

Using the brightest detection of M92B at MJD 60310, we obtained the polarization profile of M92B (shown in Figure 3), with data folded using the DSPSR package (W. van Straten & M. Bailes 2011), cleaned with the `pazi` routine, and polarization calibrated using the `pac` routine in PSRCHIVE (W. van Straten et al. 2012). We searched for a rotation measure but found no significant detection. No significant linear or circular polarization is detected at 1250 MHz, and the polarization position angle cannot be reliably determined due to the low signal-to-noise ratio.

4. Discussion

4.1. Properties of New Discovery

When M92A was first discovered, its association with M92 was inferred mainly from the agreement between its DM value and the predictions of Galactic electron density models (i.e., YMW16; J. M. Yao et al. 2017), together with its binary properties typical of GC pulsars (Z. Pan et al. 2020). A definitive confirmation was expected to require the discovery of another pulsar in the cluster with a similar DM. The newly discovered pulsar M92B has a DM consistent with that of M92A (<0.2 pc cm^{-3}), lies within the cluster core radius in projection, and exhibits a negative spin period derivative consistent with acceleration in the cluster gravitational potential (see Section 4.3). These results strongly support that both pulsars are members of M92.

The X-ray sources at 0.3–8 keV in M92 were studied in detail by T.-N. Lu et al. (2011). The closest source to M92B is

Table 1
The Timing Solution of M92B

Pulsar	J1717+4308B
R.A., α (J2000)	17:17:07.2234(1)
decl., δ (J2000)	+43:08:07.890(1)
Spin frequency, f (s^{-1})	284.78215879637(4)
Spin freq. deriv., $\dot{f}$ (s^{-2})	$2.2093(5) \times 10^{-15}$
Reference epoch (MJD)	60310.032810
Start of timing data (MJD)	58351.448
End of timing data (MJD)	60913.479
Dispersion measure, DM (pc cm^{-3})	35.292(8)
Solar system ephemeris	DE438
Terrestrial time standard	UTC (NIST)
Time units	TDB
Number of TOAs	146
Residuals rms (μs)	22.00
Binary Parameters	
Binary model	ELL1
Proj. semimajor axis, x_p (lt-s)	2.591407(3)
1st Laplace-Lagr. param., η	$6.8(2) \times 10^{-5}$
2nd Laplace-Lagr. param., κ	$-4.78(2) \times 10^{-4}$
T_{asc} (MJD)	58920.9353449(4)
Orbital period, P_b (days)	2.294099062(1)
Derived Parameters	
Spin period, P (s)	$3.5114559290740(4) \times 10^{-3}$
Spin period deriv., $\dot{P}$ (s s^{-1})	$-2.7241(6) \times 10^{-20}$
Mass function, $f(M_p)$ ($M_\odot$)	3.5502×10^{-3}
Min. companion mass, $M_{c,min}$ ($M_\odot$)	0.20
Med. companion mass, $M_{c,med}$ ($M_\odot$)	0.24
Offset in α, θ_α (arcmin)	0.0304
Offset in δ, θ_δ (arcmin)	−0.0252
Total offset, $\theta_\perp$ (arcmin)	0.0395
Dist. from center, $r_\perp$ (core radii)	0.1518
Dist. from center, $r_\perp$ (pc)	0.0953

Note. Companion mass assumes a pulsar mass of 1.35 $M_\odot$. $M_{c,min}$ and $M_{c,med}$ assume $i = 90°$ and $i = 60°$, respectively.

CX2 at R.A. = 17:17:07.296(5), decl. = +43:08:06.95(4). Its separation from the pulsar timing position is 1.″23, significantly exceeding the quoted positional uncertainties,[15] indicating the two sources are not associated. The derived binary parameters suggest that the companion star is a white dwarf or a low-mass star. We searched for an optical counterpart to this companion using data from the Hubble Space Telescope UV Globular Cluster Survey (HUGS; GO-10775, PI: Sarajedini; GO-13297, PI: Piotto; see G. Piotto et al. 2015; D. Nardiello et al. 2018).[16] We crossmatched potential counterparts across five filters (F275W, F336W, F438W, F606W, and F814W) but found no significant signal within the 3σ upper limits.

M92B was detected in 36 of 53 observations, and we derived its 1250 MHz flux densities using the radiometer equation (e.g., R. J. Dewey et al. 1985) and the FAST GC pulsar survey parameters (e.g., Z. Pan et al. 2021), obtaining a range of 0.75–4.82 μJy with a median of 2.37 μJy. The corresponding median pseudo-luminosity, $L_{1250} \sim 0.16$ mJy kpc^2, places

[15] The corresponding $\chi^2 \approx 763$, calculated from the positional offset assuming independent Gaussian uncertainties in R.A. and decl.: $\chi^2 = \left(\frac{\Delta\alpha \cos\delta}{\sigma_\alpha}\right)^2 + \left(\frac{\Delta\delta}{\sigma_\delta}\right)^2$, corresponding to a $\sim 28\sigma$ positional offset.

[16] https://archive.stsci.edu/prepds/hugs/#dataaccess

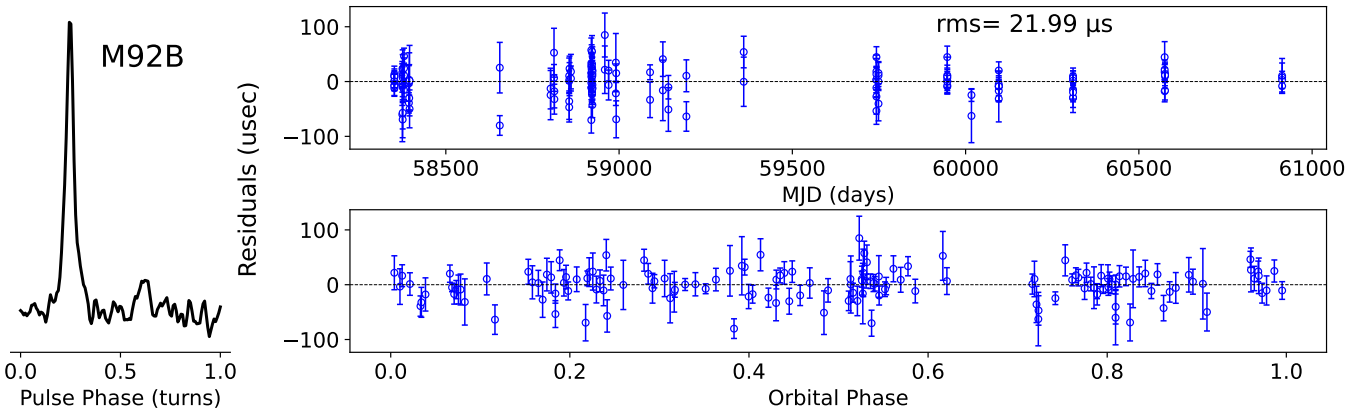

Figure 2. Average pulse profile and timing residuals of M92B. The left panel shows the integrated pulse profile obtained by summing all 36 detections over 128 phase bins. The right panel shows the timing residuals versus MJD (top) and orbital phase (bottom) from the best-fit timing model.

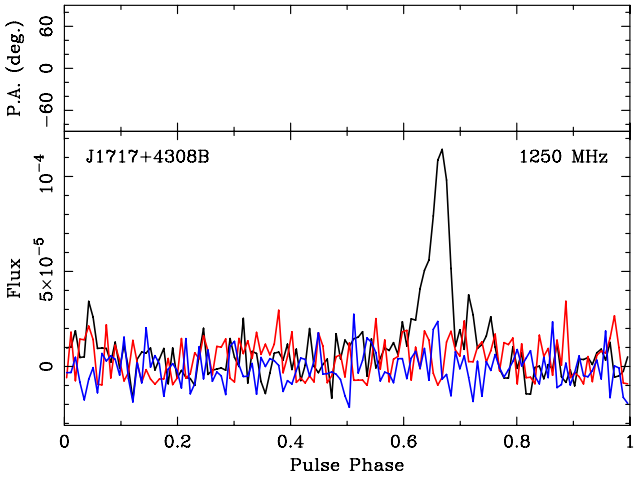

Figure 3. The polarization profile of M92B at MJD 60310. The black, red, and blue curves correspond to the total intensity (I), linear (L), and circular (V) components, respectively. The upper panel presents the position angle of the linear polarization.

M92B among the faintest binary MSPs currently known in GCs. Interstellar scintillation can occasionally boost its signal above the detection threshold, allowing us to reveal this faint binary pulsar that would otherwise remain hidden.

Its faintness and intermittent detectability indicate that additional faint MSPs may remain hidden in M92. This suggests that some pulsar-poor clusters may host substantial MSP populations dominated by sources below current detection thresholds, implying that current estimates of the GC MSP luminosity function may remain biased at the faint end (e.g., J. W. T. Hessels et al. 2007; M. Bagchi et al. 2011; J. Chennamangalam et al. 2013). Recent deep FAST searches using the power-spectrum stacking method have also revealed the presence of even fainter isolated MSP populations (Y. Dai et al. 2026). A joint analysis of the luminosity distributions of faint binary and isolated MSPs uncovered by recent deep surveys (e.g., MeerKAT and FAST) could yield new constraints on the intrinsic GC MSP population but is beyond the scope of this Letter.

Previous studies predicted a population of ∼13–43 pulsars in M92 (e.g., M. Bagchi et al. 2011; P. J. Turk & D. R. Lorimer 2013; D. Yin et al. 2024). Binary pulsars in M92 are expected to dominate the pulsar population due to the low stellar encounter rate per binary in the cluster (e.g., F. Verbunt & P. C. C. Freire 2014; K. Oh et al. 2023). If more pulsars are present, their nondetection could be due to limited sensitivity or strong orbital acceleration in compact binary systems, which reduces the effectiveness of standard periodicity searches. More computationally intensive techniques, such as phase-modulation searches (S. M. Ransom et al. 2003) and template-bank acceleration searches (V. Balakrishnan et al. 2022), may reveal highly accelerated systems in future analyses.

The small DM of pulsars in M92 implies only modest dispersion smearing even at low radio frequencies. Pulsars in GCs with typical steep radio spectra are expected to be brighter at low frequencies, therefore making sensitive low-frequency observations favorable for additional discoveries (e.g., J. Das et al. 2025, 2026). Discovering additional pulsars in M92 would not only improve the census of the cluster pulsar population but also provide new probes of the cluster potential, thereby further constraining its dynamical evolution (see Section 4.4).

4.2. Eccentricity of M92B

M92B exhibits a mildly eccentric orbit with $e \approx 4.8 \times 10^{-4}$. With $P_b \approx 2$ days and $M_c \approx 0.2\,M_\odot$, the system is consistent with the P_b–M_c relation for helium white dwarf (He WD) companions originating from low-mass X-ray binary (LMXB) evolution (T. M. Tauris & G. J. Savonije 1999). The low eccentricity magnitude disfavors an exchange origin, which typically yields $e \gtrsim 0.1$ (e.g., S. Sigurdsson & E. S. Phinney 1993), suggesting M92B is a primordial MSP–He WD system.

The initial eccentricity in MSP progenitors is expected to dissipate via tidal circularization during the LMXB phase (E. S. Phinney 1992). However, stellar interactions in dense GCs can subsequently induce nonzero eccentricities (F. A. Rasio & D. C. Heggie 1995; D. C. Heggie & F. A. Rasio 1996). Following F. A. Rasio & D. C. Heggie (1995) and R. S. Lynch et al. (2011), we estimate the timescale $t_{>e}$ required to induce the observed eccentricity as

$$t_{>e} \simeq 4 \times 10^{11}\,\mathrm{yr}\left(\frac{n}{10^4\ \ \mathrm{pc}^{-3}}\right)^{-1} \times \left(\frac{v_0}{10\ \mathrm{km\ s}^{-1}}\right)\left(\frac{P_b}{\mathrm{days}}\right)^{-2/3} e^{2/5}, \quad (1)$$

where n is the stellar number density ($n \propto \rho_0$, where ρ_0 is the central mass density of the GC), v_0 is the central stellar

velocity dispersion, P_b is the orbital period, and e is the observed eccentricity.

As a first approximation, we adopt the central mass density ρ_c and convert it to a number density via $n \approx \rho_0/\langle m_\star \rangle$, where $\langle m_\star \rangle$ is the mean stellar mass, taken to be $\sim 1\,M_\odot$ following R. S. Lynch et al. (2011). For M92B, adopting $\rho_0 \approx 1.995 \times 10^4\,L_\odot\,\mathrm{pc}^{-3}$ (W. E. Harris 2010) and $v_0 \approx 8.4\,\mathrm{km\,s}^{-1}$ (M. Libralato et al. 2022), we estimate $t_{>e} \approx 4.55$ Gyr. This timescale is shorter than the cluster age of 12.75 ± 0.25 Gyr (N. E. Q. Paust et al. 2007), indicating that dynamical perturbations are sufficient to produce the observed eccentricity.

4.3. Acceleration of M92B Caused by the Cluster Potential

The observed spin period derivative of M92B is negative ($\dot{P}_{\rm obs} < 0$). Since radio pulsars intrinsically spin down, a negative $\dot{P}_{\rm obs}$ implies that the gravitational potential of the cluster dominates the LOS acceleration of M92B (e.g., E. S. Phinney 1993). For pulsars in GCs, the observed period derivative can be written as

$$\left(\frac{\dot{P}}{P}\right)_{\rm obs} = \left(\frac{\dot{P}}{P}\right)_{\rm int} + \frac{\mu^2 d}{c} + \frac{a_{\ell,\,\rm GC}}{c} + \frac{a_g}{c}, \tag{2}$$

where μ is the total proper motion, d is the cluster distance (8.3 kpc; W. E. Harris 2010), and $\mu^2 d/c$ represents the Shklovskii effect (I. S. Shklovskii 1970). The terms $a_{\ell,\rm GC}$ and a_g denote the LOS acceleration due to the cluster potential and the differential Galactic acceleration between the solar system and the GC, respectively.

The proper motion of M92B has not yet been measured, but it is expected to be similar to that of M92. Using the Gaia EDR3 measurement of the cluster proper motion (-4.935 ± 0.024 and $-0.625 \pm 0.024\,\mathrm{mas\,yr}^{-1}$; E. Vasiliev & H. Baumgardt 2021), the Shklovskii contribution is estimated to be $\mu^2 d \approx 1.50 \times 10^{-10}\,\mathrm{m\,s}^{-2}$.

The Galactic acceleration term can be estimated following D. J. Nice & J. H. Taylor (1995) and B. J. Prager et al. (2017):

$$a_g \cdot \vec{n} = -\cos(b)\left(\frac{\Theta_0^2}{R_0}\right)\left(\cos(l) + \frac{\beta}{\sin^2(l) + \beta^2}\right), \tag{3}$$

where $R_0 = 8.34 \pm 0.16$ kpc and $\Theta_0 = 240 \pm 8\,\mathrm{km\,s}^{-1}$ are the solar Galactocentric distance and circular velocity (S. Sharma et al. 2014). Here $\beta = (d/R_0)\cos b - \cos l$, and l and b are the Galactic longitude and latitude. For M92 ($l = 68.^\circ34$, $b = 34.^\circ86$), this yields $a_g \approx -1.45 \times 10^{-10}\,\mathrm{m\,s}^{-2}$.

To estimate the cluster acceleration $a_{\ell,\rm GC}$, we adopt the analytical model derived from P. C. C. Freire et al. (2005), which assumes the spatial I. King (1962) density profile:

$$a_{\ell,\,\rm GC}(x) = \frac{9v_0^2}{d\theta_c}\frac{\ell}{x^3}\left(\frac{x}{\sqrt{1+x^2}} - \sinh^{-1}x\right), \tag{4}$$

where x is the distance from the pulsar to the center of the GC divided by its core radius ($r_c = \theta_c d$), and ℓ is the LOS offset from the cluster center, also in units of r_c. For each projected offset $\theta_\perp$, the model provides the maximum allowed LOS acceleration $a_{\ell,\rm max}$ (shown in Figure 4).

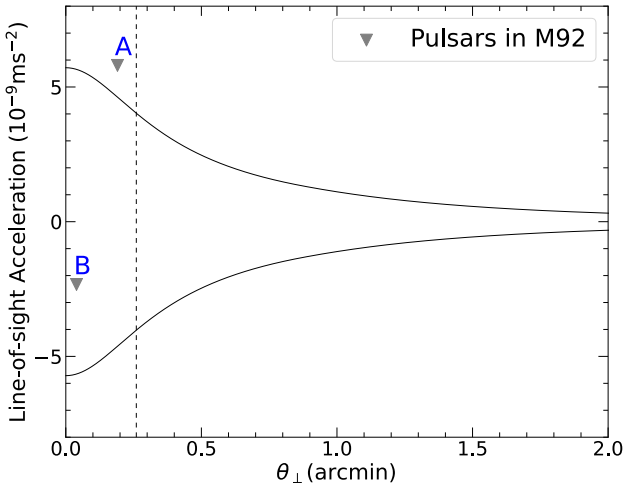

Figure 4. Acceleration model for M92. Black curves show the maximum and minimum LOS accelerations ($a_{\ell,\rm GC}$) predicted by the cluster potential as a function of projected offset ($\theta_\perp$). Downward triangles denote independent limits on pulsar accelerations ($a_{\ell,P,\rm max}$), and the vertical dashed line shows the core radius of M92 ($r_c = 0.'26$). The value of M92A is from Y. Lian et al. (2025).

An independent constraint can be derived from the observed period derivative by assuming $\dot{P}_{\rm int} = 0$:

$$a_{\ell,\rm P,max} = c\frac{\dot{P}_{\rm obs}}{P} - \mu^2 d - a_g. \tag{5}$$

For M92B we obtain $a_{\ell,\rm P,max} \approx -5.65 \times 10^{-9}\,\mathrm{m\,s}^{-2}$. The Shklovskii term and Galactic acceleration are orders of magnitude smaller than the cluster potential and the observed $c\frac{\dot{P}_{\rm obs}}{P}$ of M92B, and thus can be neglected. This suggests that the cluster gravitational potential model can well account for its negative $\dot{P}_{\rm obs}$.

Assuming the pulsar acceleration lies within $\pm a_{\ell,\rm max}$, one can derive the limits for $\dot{P}_{\rm int}$. For M92B, we obtain $\dot{P}_{\rm int} < 3.9 \times 10^{-20}\,\mathrm{s\,s}^{-1}$, corresponding to a surface magnetic field $B_s = 3.2 \times 10^{19}(P\dot{P})^{1/2}$ $G < 3.7 \times 10^8$ G and a characteristic age $\tau_c = \frac{P}{2\dot{P}} > 1.4$ Gyr. Given that the M92's age is 12.75 ± 0.25 Gyr (N. E. Q. Paust et al. 2007), the significant τ_c of M92B, compared to that of M92A ($\tau_c < 1.36$ Gyr; Y. Lian et al. 2025), implies that its real age is not constrained. Thus, we cannot exclude that M92B formed during the early stages of the cluster's evolution. This is also roughly consistent with the timescale $t_{>e} \approx 4.55$ Gyr for M92B, further indicating that this system is likely old. For binaries, orbital period derivative measurements can provide tighter constraints on cluster acceleration and intrinsic spin-down (e.g., P. C. C. Freire et al. 2017), although no significant detection is obtained with the current timing baseline. Preliminary PINT simulations (J. Luo et al. 2021) suggest that a significant detection of the expected acceleration-induced $\dot{P}_b \sim -10^{-12}$ from the cluster gravitational potential would likely require roughly another decade of timing observations.

4.4. MCMC Constraint of the Cluster Dynamics

To resolve degeneracies in photometric core parameters and provide an independent dynamical measurement of M92 from pulsars, we performed a Bayesian Markov Chain Monte Carlo (MCMC) analysis based on the framework of

B. J. Prager et al. (2017) and F. Abbate et al. (2018, 2019). We model mass segregation via a generalized pulsar number density, $n_p(r) \propto [1 + (r/r_c)^2]^{\alpha_p}$, implementing the likelihood and density modeling formalisms defined in Equations (30)–(38) of B. J. Prager et al. (2017).

The MCMC model contains seven free parameters: ρ_c, r_c, α_p, $\Delta\alpha$, $\Delta\delta$, ℓ_A, and ℓ_B, where ρ_c and r_c are the central mass density and core radius, α_p is the pulsar mass-segregation index, $\Delta\alpha$ and $\Delta\delta$ are the offsets of the trial gravitational center from the Gaia EDR3, and ℓ_A and ℓ_B are the unknown LOS positions of M92A and M92B. For each pulsar, the likelihood uses its measured sky position and LOS acceleration inferred from the observed $(\dot{P}/P)_{obs}$, after correcting for the Shklovskii term, Galactic acceleration, and a fiducial intrinsic spin-down contribution. The latter is estimated from a magnetic-dipole model with the median field–MSP magnetic field fixed at $B = 10^{8.47}$ G (B. J. Prager et al. 2017; F. Abbate et al. 2018, 2019). The sky positions determine the projected offsets from each trial cluster center and enter the spatial-density weighting, whereas the period derivatives constrain the LOS gravitational acceleration. The unknown LOS positions, ℓ_A and ℓ_B, are sampled and marginalized over.

The resulting posterior distributions (see Figure 5, corresponding to the best-fit values with 1σ errors) yield a central mass density of $\rho_c = 1.2^{+1.3}_{-0.9} \times 10^6\, M_\odot\ \mathrm{pc}^{-3}$ and a core radius of $r_c = 0.3^{+0.3}_{-0.1}$ pc. These values are in good agreement with the structural parameters derived from N-body dynamical modeling ($\rho_c = 2 \times 10^6\, M_\odot\ \mathrm{pc}^{-3}$ and $r_c = 0.29$ pc; H. Baumgardt & M. Hilker 2018) within 1σ. The inferred center-of-gravity offsets are $\Delta\alpha = 0.05^{+0.26}_{-0.19}$ arcmin and $\Delta\delta = 0.18^{+0.23}_{-0.38}$ arcmin. Both offsets are consistent with zero within 1σ, indicating that the current two-pulsar sample does not provide a statistically significant constraint on the cluster gravitational center. The pulsar mass-segregation index is $\alpha_p = -3.1^{+1.5}_{-1.2}$, consistent with the constraint of $\alpha_p = -3.56^{+0.47}_{-0.56}$ derived from 36 pulsars in Terzan 5 (B. J. Prager et al. 2017). These findings highlight the utility of pulsars as independent dynamical probes that bypass the biases of photometric measurements. As the pulsar sample in M92 grows, these fundamental structural parameters are expected to be constrained with higher precision.

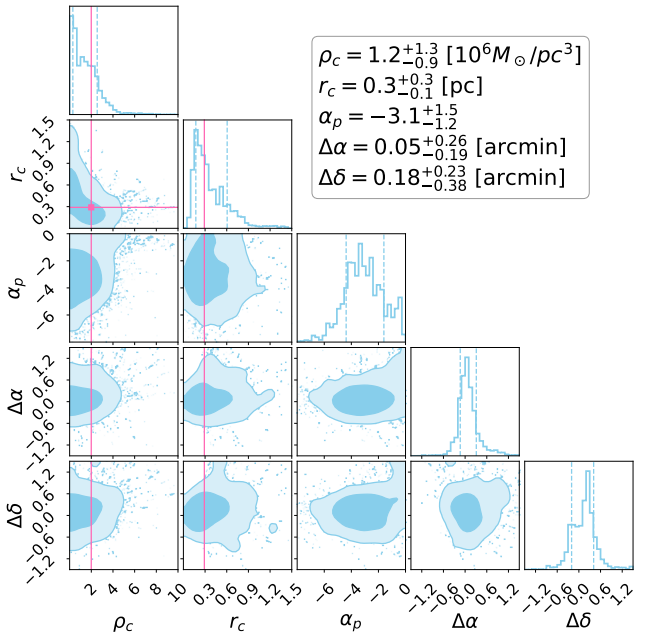

Figure 5. Marginalized posterior probability distributions for the M92 structural parameters and the offset from the gravitational center of M92 (E. Vasiliev & H. Baumgardt 2021). Parameters shown include the central mass density (ρ_c in $10^6\, M_\odot\ \mathrm{pc}^{-3}$), core radius ($r_c$ in pc), mass-segregation index of pulsars (α_p), and positional offsets from the Gaia-measured center ($\Delta\alpha$, $\Delta\delta$ in arcmin). The values shown in the legend are posterior medians with 1σ uncertainties, defined by the 16th–84th percentile range. In the 2D panels, the contours represent the 1σ and 2σ confidence level. The vertical dashed lines in the one-dimensional histograms mark the 16th and 84th percentiles, while the solid pink lines and markers denote the cluster core parameters derived from N-body dynamical modeling (H. Baumgardt & M. Hilker 2018) for comparison.

5. Conclusions

In this work, we conducted a search for additional pulsars in the GC M92 using 6 yr of FAST timing observations originally obtained for M92A. This 6 yr observational baseline significantly increases the possibility of discovering faint pulsars, particularly those intermittently detectable due to interstellar scintillation. Our main results are summarized as follows:

1. We discovered a new MSP in M92, PSR J1717+4308B (M92B). This pulsar has a spin period of 3.51 ms and resides in a binary system with an orbital period of 2.3 days and a mildly eccentric orbit ($e \simeq 4.8 \times 10^{-4}$). The minimum companion mass is $M_c \approx 0.2\, M_\odot$, suggesting a He WD companion.
2. The DM value of M92B is consistent with that of M92A (<0.2 pc cm^{-3}), its projected position lies within the cluster core radius, and its negative spin period derivative is consistent with acceleration in the cluster potential, all supporting their cluster membership.
3. No X-ray, optical, or UV band counterpart to M92B is identified. The nearest X-ray source (CX2) is positionally inconsistent, and no counterpart is detected in archival Hubble Space Telescope data down to 3σ upper limits.
4. A Bayesian MCMC analysis using M92A and M92B yields broad constraints on the core structural parameters of M92, broadly consistent with N-body dynamical modeling. This demonstrates the utility of pulsar timing for providing dynamical constraints even in clusters with very limited pulsar samples.
5. Given previous estimates of 13–43 pulsars in M92, additional pulsars likely remain undetected. If such a population indeed exists, their nondetection suggests these undiscovered sources are intrinsically faint, implying incompleteness in the faint end of the GC MSP luminosity distribution. More sensitive observations and advanced search techniques are expected to reveal further pulsars, thereby improving constraints on cluster dynamics.

Acknowledgments

This work is supported by Guizhou provincial natural science foundation project No. ZD[2026]058. Liyun Zhang has been supported by the Science and Technology Program of Guizhou Province under project Nos. QKHPTRC-ZDSYS [2023]003 and QKHFQ[2023]003. This work is also supported by the Guizhou Provincial Major Scientific and Technological Program (Nos. XKBF (2025)010 and XKBF (2025)011). This

work made use of the data from FAST (Five-hundred-meter Aperture Spherical radio Telescope) (https://cstr.cn/31116.02.FAST). FAST is a Chinese national megascience facility, operated by National Astronomical Observatories, Chinese Academy of Sciences. We gratefully acknowledge the generous computational support provided by Guizhou Suanjia Computing Services Co., Ltd, Gui'an New Area Science and Technology Innovation Industries Development Limited Company, and Gui'an Supercomputing Center. We are grateful to Dr. Zhichen Pan and Dr. Lei Qian for their guidance on pulsar searching and timing analyses, to Tong Liu and Ruili He for discussions on polarization calibration, and to Yujie Chen for help with timing simulations. Finally, we thank the anonymous referee for many constructive comments and valuable suggestions that greatly improved the clarity and quality of the manuscript.

ORCID iDs

Dejiang Yin https://orcid.org/0000-0001-6051-3420
Li-yun Zhang https://orcid.org/0000-0002-2394-9521
Baoda Li https://orcid.org/0009-0008-4109-744X
Yinfeng Dai https://orcid.org/0009-0007-6396-7891
Lin Wang https://orcid.org/0000-0003-0757-3584
Qiuyu Yu https://orcid.org/0009-0002-2059-6350
Yujie Lian https://orcid.org/0009-0001-6693-7555

References

Abbate, F., Possenti, A., Colpi, M., & Spera, M. 2019, ApJL, 884, L9
Abbate, F., Possenti, A., Ridolfi, A., et al. 2018, MNRAS, 481, 627
Alpar, M. A., Cheng, A. F., Ruderman, M. A., & Shaham, J. 1982, Natur, 300, 728
Andersen, B. C., & Ransom, S. M. 2018, ApJL, 863, L13
Bagchi, M., Lorimer, D. R., & Chennamangalam, J. 2011, MNRAS, 418, 477
Balakrishnan, V., Champion, D., Barr, E., et al. 2022, MNRAS, 511, 1265
Barr, E. D., Dutta, A., Freire, P. C. C., et al. 2024, Sci, 383, 275
Baumgardt, H., & Hilker, M. 2018, MNRAS, 478, 1520
Camilo, F., Lorimer, D. R., Freire, P., Lyne, A. G., & Manchester, R. N. 2000, ApJ, 535, 975
Chennamangalam, J., Lorimer, D. R., Mandel, I., & Bagchi, M. 2013, MNRAS, 431, 874
Clark, G. W. 1975, ApJL, 199, L143
Corongiu, A., Ridolfi, A., Abbate, F., et al. 2024, ApJ, 972, 198
Dai, Y., Zhu, X.-J., Pan, Z., et al. 2026, ApJL, 1002, L31
Das, J., Roy, J., Freire, P. C. C., et al. 2025, ApJ, 988, 161
Das, J., Roy, J., Freire, P. C. C., et al. 2026, ApJ, 1000, 116
Dewey, R. J., Taylor, J. H., Weisberg, J. M., & Stokes, G. H. 1985, ApJL, 294, L25
Freire, P. C., Kramer, M., Lyne, A. G., et al. 2001, ApJL, 557, L105
Freire, P. C. C., Hessels, J. W. T., Nice, D. J., et al. 2005, ApJ, 621, 959
Freire, P. C. C., & Ridolfi, A. 2018, MNRAS, 476, 4794
Freire, P. C. C., Ridolfi, A., Kramer, M., et al. 2017, MNRAS, 471, 857
Harris, W. E. 2010, arXiv:1012.3224
Heggie, D. C., & Rasio, F. A. 1996, MNRAS, 282, 1064
Hessels, J. W. T., Ransom, S. M., Stairs, I. H., et al. 2006, Sci, 311, 1901
Hessels, J. W. T., Ransom, S. M., Stairs, I. H., Kaspi, V. M., & Freire, P. C. C. 2007, ApJ, 670, 363
Hotan, A. W., van Straten, W., & Manchester, R. N. 2004, PASA, 21, 302
Jiang, P., Tang, N.-Y., Hou, L.-G., et al. 2020, RAA, 20, 064
Jiang, P., Yue, Y., Gan, H., et al. 2019, SCPMA, 62, 959502
King, I. 1962, AJ, 67, 471
Lange, C., Camilo, F., Wex, N., et al. 2001, MNRAS, 326, 274
Li, Y., Wang, L., Qian, L., et al. 2025, ApJ, 991, 38
Lian, Y., Pan, Z., Zhang, H., et al. 2025, ApJS, 279, 51
Libralato, M., Bellini, A., Vesperini, E., et al. 2022, ApJ, 934, 150
Lorimer, D. R., & Kramer, M. 2004, Handbook of Pulsar Astronomy, Vol. 4 (Cambridge Univ. Press)
Lu, T.-N., Kong, A. K. H., Verbunt, F., et al. 2011, ApJ, 736, 158
Luo, J., Ransom, S., Demorest, P., et al. 2021, ApJ, 911, 45
Lynch, R. S., Ransom, S. M., Freire, P. C. C., & Stairs, I. H. 2011, ApJ, 734, 89
Nan, R., Li, D., Jin, C., et al. 2011, IJMPD, 20, 989
Nardiello, D., Libralato, M., Piotto, G., et al. 2018, MNRAS, 481, 3382
Nice, D., Demorest, P., Stairs, I., et al. 2015, Tempo: Pulsar timing data analysis, Astrophysics Source Code Library, ascl:1509.002
Nice, D. J., & Taylor, J. H. 1995, ApJ, 441, 429
Oh, K., Hui, C. Y., Hong, J., et al. 2023, MNRAS, 525, 4167
Pan, Z., Qian, L., Ma, X., et al. 2021, ApJL, 915, L28
Pan, Z., Ransom, S. M., Lorimer, D. R., et al. 2020, ApJL, 892, L6
Paust, N. E. Q., Chaboyer, B., & Sarajedini, A. 2007, AJ, 133, 2787
Perera, B. B. P., Stappers, B. W., Lyne, A. G., et al. 2017, MNRAS, 468, 2114
Phinney, E. S. 1992, RSPTA, 341, 39
Phinney, E. S. 1993, ASPC, 50, 141
Piotto, G., Milone, A. P., Bedin, L. R., et al. 2015, AJ, 149, 91
Prager, B. J., Ransom, S. M., Freire, P. C. C., et al. 2017, ApJ, 845, 148
Ransom, S. M. 2001, PhD thesis, Harvard Univ.
Ransom, S. M. 2008, IAUS, 246, 291
Ransom, S. M., Cordes, J. M., & Eikenberry, S. S. 2003, ApJ, 589, 911
Ransom, S. M., Eikenberry, S. S., & Middleditch, J. 2002, AJ, 124, 1788
Ransom, S. M., Hessels, J. W. T., Stairs, I. H., et al. 2005, Sci, 307, 892
Rasio, F. A., & Heggie, D. C. 1995, ApJL, 445, L133
Ridolfi, A., Gautam, T., Freire, P. C. C., et al. 2021, MNRAS, 504, 1407
Sharma, S., Bland-Hawthorn, J., Binney, J., et al. 2014, ApJ, 793, 51
Shklovskii, I. S. 1970, SvA, 13, 562
Sigurdsson, S., & Phinney, E. S. 1993, ApJ, 415, 631
Tauris, T. M., & Savonije, G. J. 1999, A&A, 350, 928
Taylor, J. H. 1992, RSPTA, 341, 117
Turk, P. J., & Lorimer, D. R. 2013, MNRAS, 436, 3720
van Straten, W., & Bailes, M. 2011, PASA, 28
van Straten, W., Demorest, P., & Oslowski, S. 2012, AR&T, 9, 237
Vasiliev, E., & Baumgardt, H. 2021, MNRAS, 505, 5978
Verbunt, F., & Freire, P. C. C. 2014, A&A, 561, A11
Yao, J. M., Manchester, R. N., & Wang, N. 2017, ApJ, 835, 29
Yin, D. 2025, Multiple Observation Segment Search (MOSS) for Pulsars, v1.0.1, Zenodo, doi:10.5281/zenodo.20178378
Yin, D., Wang, L., Zhang, L.-y., et al. 2025, ApJ, 991, 177
Yin, D., Zhang, L.-y., Qian, L., et al. 2024, ApJL, 969, L7
Yin, D.-J., Zhang, L.-Y., Li, B.-D., et al. 2023, RAA, 23, 055012
Zhang, L., Hobbs, G., Li, D., et al. 2016, RAA, 16, 151
Zhao, J., & Heinke, C. O. 2022, MNRAS, 511, 5964